Impact of land-use changes on soil hydraulic properties of Calcaric Regosols on the Loess Plateau, NW China

Miaozi Yu[1,2], Lulu Zhang[2,3], Xuexuan Xu[4]*, Karl-Heinz Feger[2], Yanhui Wang[5], Wenzhao Liu[4], and **Kai Schwärzel[3]**

[1] Northwest A&F University, College of Resources and Environment, Yangling, Shaanxi, 712100, China
[2] Technische Universität Dresden, Institute of Soil Science and Site Ecology, Faculty of Environmental Sciences, Pienner Straße 19, 01737 Tharandt, Germany
[3] United Nations University, Institute for Integrated Management of Material Fluxes and of Resources (UNU-FLORES), Ammonstraße 74, 01067 Dresden, Germany
[4] Northwest A&F University, Institute of Soil and Water Conservation, Yangling, Shaanxi, 712100, China
[5] Chinese Academy of Forestry, Research Institute of Forest Ecology, Environment and Protection, Beijing 100091, China

Abstract

Vegetation restoration efforts (planting trees and grass) have been effective in controlling soil erosion on the Loess Plateau (NW China). Shifts in land cover result in modifications of soil properties. Yet, whether the hydraulic properties have also been improved by vegetation restoration is still not clear. The objective of this paper was to understand how vegetation restoration alters soil structure and related soil hydraulic properties such as permeability and soil water storage capacity. Three adjacent sites with similar soil texture, soil type, and topography, but different land cover (black locust forest, grassland, and cropland) were selected in a typical small catchment in the middle reaches of the Yellow River (Loess Plateau). Seasonal variation of soil hydraulic properties in topsoil and subsoil were examined. Our study revealed that land-use type had a significant impact on field-saturated, near-saturated hydraulic conductivity, and soil water characteristics. Specifically, conversion from cropland to grass or forests promotes infiltration capacity as a result of increased saturated hydraulic conductivity, air capacity, and macroporosity. Moreover, conversion from cropland to forest tends to promote the creation of mesopores, which increase soil water-storage capacity. Tillage of cropland created temporarily well-structured topsoil but compacted subsoil as indicated by low subsoil saturated hydraulic conductivity, air capacity, and plant-available water capacity. No impact of land cover conversion on unsaturated hydraulic conductivities at suction > 300 cm was found indicating that changes in land cover do not affect functional meso- and microporosity. Our work demonstrates that changes in soil hydraulic properties resulting from soil conservation efforts need to be considered when soil conservation measures shall be implemented in water-limited regions. For ensuring the sustainability of such measures, the impact of soil conversion on water resources and hydrological processes needs to be further investigated.

Key words: hydraulic conductivity / land-use change / Loess Plateau / tillage / water retention curve

Accepted March 10, 2015

1 Introduction

The Loess Plateau of NW China suffers severe soil erosion resulting from intense summer showers and instable slopes, which is a consequence of deforestation, overgrazing, and intensified cultivation. Soil erosion rates between 10,000 and 25,000 t km^{-2} y^{-1} have been reported for this region (*Zhang* et al., 1998). The large amount of sediment loaded into the Yellow River causes the riverbed to rise and increases risks of flood in the middle and lower reaches of the Yellow River. To control soil erosion in the loess region, large-scale vegetation restoration (*i.e.*, afforestation), building of slope terraces, and check-dams (sediment-trapping dams) have been implemented since the late 1950s on the Loess Plateau (*Zhang* et al., 2014; *Cao*, 2008; *Zhou* et al., 2012). These modifications in vegetation and landform may alter soil properties including soil hydraulic properties. Soil hydraulic properties control transport of water and nutrients in soil. They are often recognized as soil quality indicator and important parameters in soil erosion studies (*Boix-Fayos* et al., 2001; *Springer* and *Cundy*, 1988). Additionally, knowledge of soil hydraulic properties is also vital for simulation of water movement (*e.g.*, infiltration, conductivity, storage, and plant-water relationships) for management purposes. Thus, it is of great importance to understand if and how the vegetation restoration affects the soil physical properties. At the same time, it also may give implications for better adaptive measures for environmental restoration practices.

* Correspondence: X. Xu; e-mail: xuxuexuan@nwsuaf.edu.cn

It is expected that changes in land use will affect soil aggregates, pore continuity, size and volume, bulk density, and organic matter, and thus may strongly influence the hydraulic properties of soil. To date, studies dealing with the effect of changing land use and management on soil hydraulic properties remain rare, especially subsoil properties (*Shukla* et al., 2003; *Stolte* et al., 2003; *Schwärzel* et al., 2011). Although soil water infiltration has been measured in several studies on the Loess Plateau (*Hu* et al., 2009, 2012; *Zhang* et al., 2011), a thorough investigation on the impact of conversion of cropland to forests or grassland on soil hydraulic properties has not been conducted. To fill the research gap, the objective of our work was to gain a better understanding of the impact of vegetation restoration on field-saturated and unsaturated hydraulic conductivities as well as on soil water retention curves in both topsoil and subsoil. For this purpose, three different kinds of land use (forest, grassland, and cropland) were selected. Our hypothesis was that before the shift in land cover the initial soil structure of the three sites was similar and the observed differences in soil hydraulic properties were caused by conversion in land cover.

2 Material and methods

2.1 Study site

Zhonggou catchment (35°20′N, 107°31′E), a small catchment in the semi-humid gully region of the Loess Plateau in the upper reaches of the Jing River (Gansu Province, NW China), was selected as study area. The catchment is ≈14 km^2 in size with an elevation ranging between 1000 and 1300 m asl. The stream drains into the Jing River, which is one of the major tributaries in the middle reaches of the Yellow River. The average annual precipitation is 509 mm y^{-1}, with 60% of the annual precipitation occurring from July to September. The annual mean temperature and potential evapotranspiration are 10.2°C and 1394 mm y^{-1}, respectively (values based on long-term observation during 1956–2010 at the Jingchuan weather station located 14 km W of the study site). The catchment is covered by loess deposits with 50 to 80 m in thickness. The soil is classified as Calcaric Regosol (*WRB*, 2006) with a texture of silt loam (for detailed soil information see Table 1).

Three main kinds of land use exist at this site: forest, grassland, and cropland. In Zhonggou, a large-scale afforestation program was conducted in the 1980s due to soil conservation. Before the afforestation, most of the land in the catchment was used for crop production. After the afforestation, 83% of the land is covered by plantation of black locust (*Robinia pseudoacacia* L.). Part of the remaining cropland area was abandoned and allowed grasses to grow naturally. The dominant species in the grassland include *Artemisia argyi* H. Lév. & Vaniot, *Pennisetum centrasiaticum* Tzvelev, *Arundinella anomala* Steud., *Achnatherum sibiricum* (L.) Keng ex Tzvelev, *Jasminum nudiflorum* Lindl., *Medicago minima* (L.) Grufberg, and *Tripolium vulgare* Nees. Forest and grassland were not disturbed by human activities. On cropland, rape (*Brassica napus* L.) was planted with a 3 y rotation (winter wheat / rape–winter wheat / rape–maize). In addition, conventional tillage was applied with a maximum depth of 30 cm.

2.2 Field measurements

2.2.1 Saturated and near-saturated hydraulic conductivity

The field measurements were conducted under black locust plantation, grass, and rape cultivation in June and September 2012 and March 2013. For the cropland, the measurements were carried out 2 weeks after harvesting, 2 weeks after sowing, and during the flowering phase of rape. All of the selected measurement plots were adjacent (less than 1000 m away from the others), and had similar topography (loess tableland), weather conditions, and soil properties (Table 1). In surface soil (0 cm) and subsoil (at 30 cm depth) saturated and near-saturated hydraulic conductivity (five replicates for each depth and treatment per measuring time) were determined using a hood infiltrometer (UGT Müncheberg, Germany). This is a special type of a tension infiltrometer, which is a valuable tool for measuring the soil hydraulic conductivity at and near saturation and has been used in many studies (*Scheffler* et al., 2011; *Schwärzel* et al., 2011; *Schwärzel* and *Punzel*, 2007). Compared to other methods, with hood infiltrometer there is no need for providing a contact layer on the measuring surface or any preparation of the soil except for avoiding air entry through the side walls.

Table 1: Basic properties of the soils investigated at the sites with contrasting land use (Zhonggou catchment, Gansu Province, NW China). The soil type is a Calcaric Regosol, the parent material is loess. SOC = soil organic carbon content; EC = electrical conductivity. Sand: 2000–63 μm, silt: 63–2 μm, clay: < 2 μm.

Site	Land use / Vegetation	Depth / cm	Horizon	Sand / %	Silt / %	Clay / %	SOC / %	N / %	$CaCO_3$ / %	pH (H_2O)	EC / dS m^{-1}
Forest	Black locust	0–6	A_1	0.4	82.2	17.4	0.66	0.08	13.6	8.3	0.90
	(*Robinia pseudoaccacia* L.)	30–36	A_2	1.0	83	16	0.34	0.04	16.7	8.4	0.82
Grassland	Grassland	0–6	A_1	1.3	80.8	17.9	0.79	0.07	13.4	8.4	0.84
	(after cropland)	30–36	A_2	1.0	81.6	17.4	0.29	0.05	15.0	8.4	0.76
Cropland	Rape	0–6	A_{p1}	1.1	79.4	19.6	0.86	0.10	6.7	8.3	0.97
	(*Brassica napus* L.)	30–36	A_{p2}	1.0	78.8	20.2	0.87	0.10	6.5	8.3	1.18

The following pressure heads were applied: 0, –1, –2, and –3 cm (1 cm of water = 0.09807 kPa). In total 90 infiltration measurements at four different pressure heads were conducted between June 2012 and March 2013. Details for the set-up of the hood infiltrometer are given by *Schwärzel* and *Punzel* (2007). The analysis of the hood infiltrometer measurements is based on *Wooding's* (1968) solution for infiltration from a circular source with a constant pressure head at the soil surface. The unsaturated hydraulic conductivity $K(h_0)$ is given by an exponential function (*Gardner* 1958):

$$K(h_0) = K_S \exp(\alpha_{GE} h_0) \quad h_0 \leq 0\,, \tag{1}$$

where K_S (L T^{-1}) is the saturated hydraulic conductivity, and α_{GE} (L^{-1}) is the slope of the ln*K versus h* [pressure head (L)] curve, and h_0 (L) is the applied pressure head, then the steady-state flow rate Q (L^3 T^{-1}) is given by:

$$Q = \pi b^2 K(h_0) + \frac{4b}{\alpha_{GE}} K(h_0)\,, \tag{2}$$

where b (L) is the radius of the infiltration surface, and $K(h_0)$ is the unsaturated hydraulic conductivity at pressure head h_0. Equation (2) can be solved for $K(h_0)$ using multiple pressure heads for a given hood radius, whereby Eq. (1) and (2) are applied piecewise such that α_{GE} is a constant in the interval between two successively applied pressure heads.

2.2.2 Water-conducting porosity

The maximum water-filled pore size at a specific pressure head can be calculated from the capillary rise equation:

$$r = -\frac{2\sigma\cos\beta}{\rho g h} \approx -\frac{0.15}{h}\,, \tag{3}$$

where r is the radius of the pore (L), σ is the surface tension of water (MT^{-2}), β is the contact angle between water and the pore wall, ρ is the density of water (ML^{-3}), g is the acceleration as a result of gravity (LT^{-2}) and h is the applied water pressure head (L). In this study we used the pressure head of –1, –2, and –3 cm to calculate the radius of the pores.

The water-conducting porosity is given by *Watson* and *Luxmoore* (1986):

$$N = \frac{8\mu K}{\pi\rho g (r)^4}\,, \tag{4}$$

$$\theta = N\pi r^2 = \frac{8\mu K}{\rho g r^2}\,, \tag{5}$$

where N is the number of pores per unit soil surface, μ is the viscosity of water (ML^{-1} T^{-1}), K is the hydraulic conductivity (L T^{-1}) obtained for two consecutive pressure heads, r is the given radius of the pore (L), and θ is water-conducting porosity (%).

2.2.3 The contribution of each pore class to the flow

The contribution of each pore class to the flow φ_i (%) was calculated according to *Watson* and *Luxmoore* (1986):

$$\varphi_i(\%) = \frac{K(\varphi_i) - K(\varphi_{i-1})}{K_s} \times 100, i = 1, \ldots, n, \tag{6}$$

where n is the number of measurements performed in a sequence, φ is the pressure head, $K(\varphi_i)$–$K(\varphi_{(i-1)})$ are the hydraulic conductivities obtained for two consecutive pressure heads, and K_s is the saturated hydraulic conductivity.

2.2.4 Fine root density

Soil cores (10 cm in diameter and height) were extracted in June 2012 at 0–10, 10–20, 20–30, 30–40, 40–50, and 50–60 cm. For each land use, 10 soil cores were randomly sampled at every depth in a 5 m × 5 m plot. The living fine roots (diameter < 2 mm) were carefully separated from soil by hand. After washing free of soil, the roots were oven-dried at 70°C for 24 h and weighed. The fine root mass density was calculated as the root mass divided by the inner volume of the soil cores.

2.3 Laboratory measurements

Following all infiltration experiments, we extracted undisturbed soil cores (6 cm in height, 250 cm^3 in volume), from beneath the positions where the infiltration had been measured. In total, 90 samples were taken between June 2012 and March 2013. Unsaturated hydraulic conductivity was determined using the evaporation method according to *Schindler* (1980). In a first step, we determined the soil water retention at the soil pressure heads of –10 (equal to pF = 1), –20 (pF = 1.3), and –31 cm (pF = 1.5). For this, samples were placed into a tray that held enough deaerated water to nearly cover them and allowed soil to soak until saturated. The dewatering process was performed using ceramic plates connected to a hanging water column. Upon completion of the measurement at the pressure head of –31 cm, two mini-tensiometers (diameter 2 mm and 65 mm length of the ceramic cup) were installed at depths of 1.5 and 4.5 cm and connected to pressure transducers with a precision of ± 1 cm. Then, the lid-covered cores were placed onto impermeable plates for the evaporation experiments. After equilibration, immediately before the evaporation experiments, tensiometer readings were compared and corrected, assuming that hydraulic equilibrium had been reached (*Schwärzel* et al., 2006). The evaporation experiment was then started; pressure heads and the weights of the cores were automatically recorded every 30 min using the ku-pF-apparatus (UGT Müncheberg, Germany). At the end of the experiments, tensiometers were removed from the cores. The residual water contents of the cores were determined by oven-drying at 105°C and weighed.

In addition, repacked small cores (volume 8 cm^3) were used to determine the gravimetric water content at pF = 4.2 using a pressure cell (Soil Moisture Equipment Corp., Santa Barbara, CA, USA). The soil of these repacked cores was sampled from beneath the positions where the infiltration had been measured. Water retention and conductivity data were described with the van Genuchten–Mualem (VGM) model (*van Genuchten*, 1980; *Mualem*, 1976):

$$\theta(h) = \theta_r + \frac{\theta_s - \theta_r}{(1 + |\alpha h|^n)^m}\,, \quad (7)$$

$$K(S_e) = K_s S_e^{1/2}[1 - (1 - S_e^{1/m})^m]^2 (m = 1 - 1/n)\,, \quad (8)$$

where θ is the volumetric water content ($L^3\ L^{-3}$), θ_r and θ_s are the residual and saturated water contents ($L^3\ L^{-3}$) respectively, h is the pressure head (L), α (L^{-1}) and n (–) are parameters, K_s is the saturated hydraulic conductivity ($L\ T^{-1}$), and S_e (–) is the effective saturation ($S_e = \frac{\theta - \theta_r}{\theta_s - \theta_r}$).

Field capacity was determined as the water content retained in soil at pF = 2.5; air capacity was determined as the volume between pF = 0 and pF = 2.5; plant-available water capacity is the water stored between pF = 2.5 and pF = 4.2; the permanent wilting point is the water content at pF = 4.2.

For each soil sample, bulk density was determined from undisturbed soil core cylinders. Afterwards, the soil samples were dried at 40°C and sieved with a mesh size of 2 mm. Contents of C and N were determined usinga Vario EL III (Elementar, Hanau, Germany). A combination of sieve method and sedimentation method with pipette apparatus was used for the determination of soil-particle size distribution. A Scheibler calcimeter (Eijkelkamp, Giesbeek, The Netherlands) was used to determine the content of Ca-carbonate ($CaCO_3$). In addition, pH (using thermal compensated pH-electrode) and electrical conductivity (using conductometer) were also measured.

2.4 Data statistics

The geometric mean, standard deviation, and coefficient of variation of the five repetitions of the saturated and near-saturated hydraulic conductivity, were calculated for data description and comparison. Additionally, analysis of variance (ANOVA) was implemented (α = 0.05 for a 95% confidence) to compare the differences of soil properties between land uses and seasons. As essential prerequisites for ANOVA, homogeneity of variance test (Levene's test) and normal distribution test (Shapiro–Wilk test) were carried out to ensure the accuracy of the analysis.

3 Results and discussion

3.1 Saturated and near-saturated hydraulic conductivity

Saturated and near-saturated hydraulic conductivity data for different land uses, depths, and seasons are listed in Table 2.

Table 2: Saturated and near-saturated hydraulic conductivity (both determined in the field using the hood infiltrometer) as well as unsaturated hydraulic conductivity (measured in the lab using the evaporation method) for different plant cover at different measuring times. In brackets: coefficients of variation (%). Zhonggou catchment, Gansu province, NW China. Basic soil properties are given in Table 1.

Measuring Time	Land use	Depth	Hydraulic conductivity (cm d^{-1}) at water pressure head of							
		cm	0 cm	–1 cm	–2 cm	–3 cm	–100 cm	–300 cm	–500 cm	–700 cm
June 2012	Forest	0–6	1111 (56)	914 (54)	752 (53)	618 (51)	0.1172 (49)	0.0084 (69)	0.0027 (90)	0.0012 (114)
		30–36	242 (75)	205 (64)	173 (56)	146 (49)	0.0940 (48)	0.0177 (11)	0.0079 (12)	0.0042 (22)
	Grassland	0–6	2902 (30)	2165 (31)	1616 (35)	1206 (39)	0.0816 (84)	0.0096 (63)	0.0040 (55)	0.0021 (50)
		30–36	371 (33)	322 (31)	279 (30)	242 (28)	0.1664 (36)	0.0182 (29)	0.0071 (44)	0.0036 (61)
	Cropland	0–6	801 (27)	558 (45)	388 (63)	270 (81)	0.1168 (9)	0.0339 (6)	0.0206 (13)	0.0143 (19)
		30–36	49 (81)	39 (70)	31 (61)	25 (54)	0.0655 (26)	0.0118 (41)	0.0055 (52)	0.0030 (62)
Sep. 2012	Forest	0–6	2103 (37)	1764 (38)	1480 (39)	1242 (41)	0.0727 (61)	0.0118 (44)	0.0056 (43)	0.0032 (47)
		30–36	223 (113)	194 (128)	169 (145)	147 (163)	0.1643 (23)	0.0183 (48)	0.0070 (58)	0.0034 (64)
	Grassland	0–6	3010 (16)	2382 (14)	1886 (14)	1492 (17)	0.0916 (36)	0.0195 (32)	0.0100 (37)	0.0061 (46)
		30–36	274 (104)	226 (101)	186 (98)	153 (96)	0.1995 (21)	0.0242 (13)	0.0097 (14)	0.0049 (18)
	Cropland	0–6	2060 (32)	1029 (44)	514 (65)	257 (93)	0.0881 (54)	0.0157 (10)	0.0075 (12)	0.0043 (18)
		30–36	51 (36)	46 (31)	43 (28)	39 (25)	0.0821 (60)	0.0134 (76)	0.0056 (76)	0.0029 (75)
March 2013	Forest	0–6	865 (48)	693 (46)	541 (48)	429 (48)	0.1091 (82)	0.0165 (29)	0.0074 (15)	0.0041 (30)
		30–36	98 (132)	82 (124)	69 (116)	57 (107)	0.0758 (197)	0.0112 (138)	0.0049 (115)	0.0027 (100)
	Grassland	0–6	1819 (42)	1407 (45)	1129 (52)	906 (61)	0.0785 (26)	0.0099 (35)	0.0042 (42)	0.0022 (49)
		30–36	358 (67)	307 (66)	260 (67)	233 (67)	0.2039 (38)	0.0191 (1)	0.0066 (19)	0.0030 (33)
	Cropland	0–6	756 (44)	562 (30)	417 (21)	310 (24)	0.0781 (87)	0.0083 (90)	0.0033 (91)	0.0017 (91)
		30–36	62 (88)	55 (74)	49 (62)	44 (56)	0.1215 (50)	0.0155 (40)	0.0061 (37)	0.0030 (35)

In the topsoil, saturated conductivities ranged between 756 and 3010 cm d^{-1}, the subsoil between 49 and 371 cm d^{-1}. It is clear that the topsoil had much higher saturated and near-saturated conductivity than the subsoil; this is mainly due to more soil organic carbon and fine root density as well as lower soil bulk density in the topsoil (Tables 1 and 3, Fig. 1). In comparison to our measurements, *Hu* et al. (2009) observed a much smaller field saturated hydraulic conductivity for the topsoil of a sandy loam-textured loess soil. Their values ranged between 47 and 396 cm d^{-1}. A possible reason for the discrepancies might be that *Hu* et al. (2009) determined the conductivity using a disc infiltrometer. It is recognized that

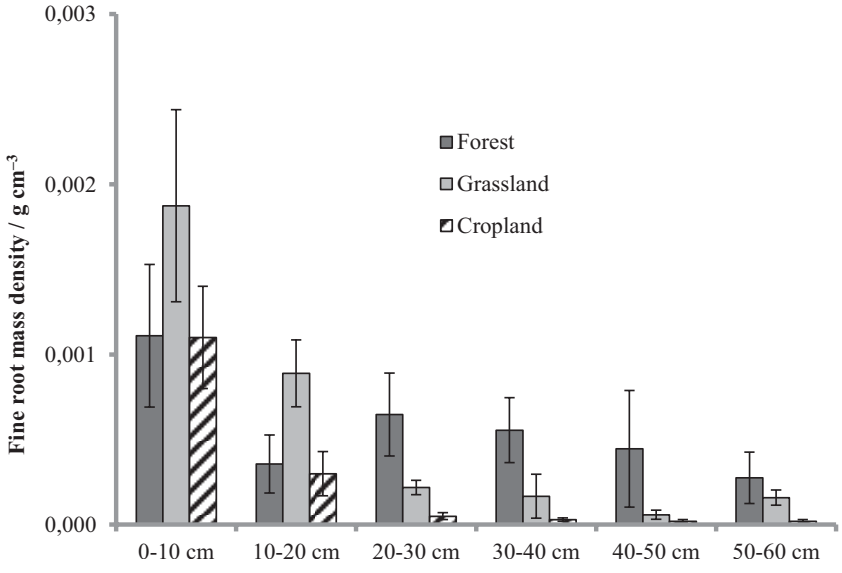

Figure 1: Fine root mass density in each 10 cm depth interval under forest, grassland, and cropland in June. The vertical bars on the graph represent the standard deviation of ten parallel measurements.

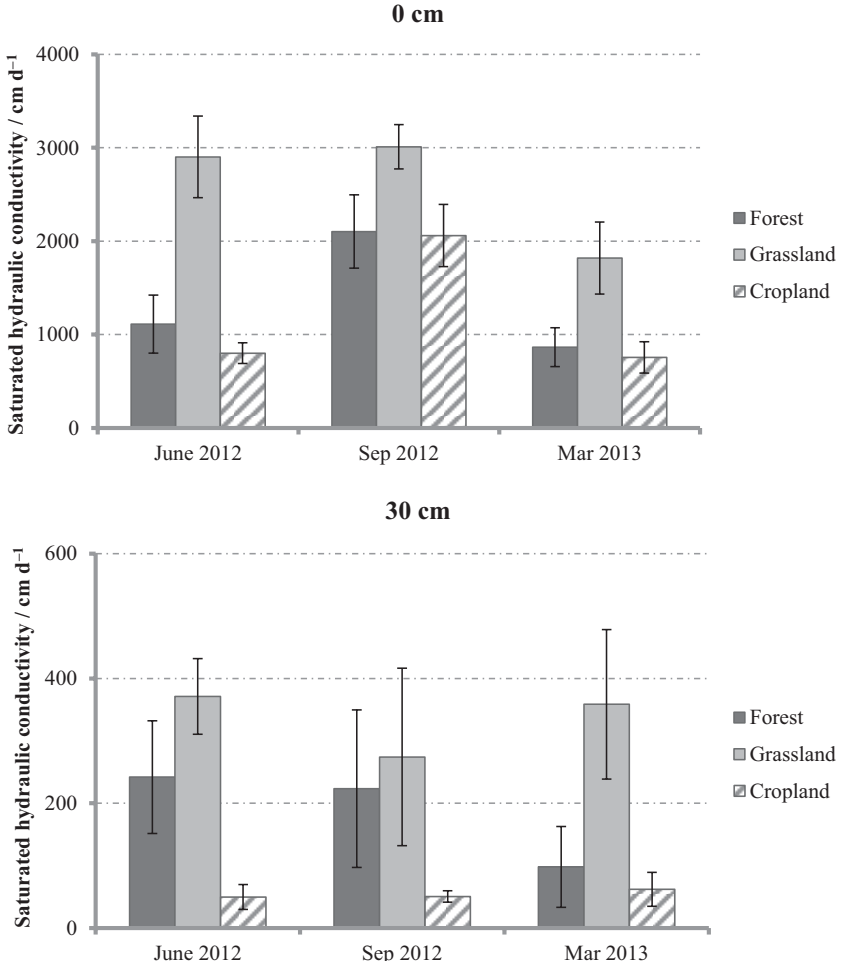

Figure 2: Soil saturated hydraulic conductivity under forest, grassland, and cropland in June and September 2012 and March 2013. The top graph shows the topsoil data, below the data of the soil depth at 30 cm. The vertical bars on the graph represent the standard deviation of five parallel measurements.

such devices require a complete hydraulic contact between the membrane of the infiltrometer chamber and the soil (*Angulo-Jaramillo* et al., 2000). To achieve this contact, the soil must be leveled and covered with a material that has a greater hydraulic conductivity than the soil. The contact layer can cause a substantial discrepancy between the pressure head set on a tension infiltrometer membrane and the pressure head at the soil surface (*Reynolds* and *Zebchuk*, 1996), and/or may smear, seal, or clog macropores (*Schwärzel* and *Punzel*, 2007). As a result, the field saturated hydraulic conductivity might be underestimated. *Zhang* et al. (2007) used the Guelph permeameter for determining the field saturated hydraulic conductivity of a silty loam soil at an agricultural site on the Loess Plateau. Their measurements were conducted at depths from 10 to 80 cm. The subsoil conductivities ranged between 50 and 152 cm d^{-1}, which have a similar range as our subsoil conductivities.

According to our measurements, land-use types had a significant effect on field saturated and near-saturated hydraulic conductivity in both the topsoil and subsoil (Table 2). In all of the three measuring campaigns, saturated conductivity was always highest under grassland and lowest under cropland (Fig. 2) implying that there was a larger number of pores and greater pore continuity under grassland, which is also demonstrated by the higher air capacity (AC) (Table 3). This finding is similar to that of *Bodhinayake* and *Cheng Si* (2004) who reported that macro-porosity and total porosity under grass were significantly larger than under cropland. These differences in porosity led to differences in hydraulic conductivity: the saturated conductivity under grass was up to three times larger than under cultivated land (*Bodhinayake* and *Cheng Si*, 2004). Our results of conductivity were also in agreement with the visual soil profile description. In comparison to the soils under cropland and forest, more fine roots (Fig. 1), desiccation cracks, and animal burrows were observed under grass, indicating a more macropore-rich soil structure. This soil structure led to lower bulk densities of grassland soil in comparison to the cropland or forest soil (Table 3).

Soil saturated and near-saturated hydraulic conductivity was subject to seasonal variation. ANOVA analysis indicates that this variation was statistically significant in the topsoil but insignificant in the subsoil (Table 4). Figure 2 shows that the saturated hydraulic conductivity increased in June and September but decreased in March under forest and grass. This can be explained in terms of increased activity of plant roots and soil fauna during the season. The rain falls mainly from July to September, thus the soil water content usually is high enough and the temperature is close to the optimum living

Table 3: Mean values of bulk density, porosity, air capacity (AC), field capacity (FC), plant available water capacity (PAWC), and permanent wilting point (PWP) of forest, grassland, and cropland sites on the Loess Plateau (NW China). Samples were taken during three campaigns (June, September 2012, and March 2013). In brackets: coefficients of variation (%).

Site	Measuring Time	Depth cm	Bulk density / g cm^{-3}	AC (pF 0–2.5) / cm^3 cm^{-3}	FC (pF 2.5)	PAWC (pF 2.5–4.2)	PWP (pF 4.2)
June 2012	Forest	0–6	1.19 (12.94)	18.8 (21.6)	29.2 (6.6)	15.4 (7.3)	13.8 (12.5)
		30–36	1.38 (4.70)	13.3 (31.8)	28.7 (9.4)	15.2 (14.5)	13.5 (5.3)
	Grassland	0–6	1.04 (6.99)	21.2 (5.9)	25.6 (3.8)	11.1 (7.7)	14.5 (7.9)
		30–36	1.26 (2.04)	18.0 (7.1)	26.4 (3.5)	15.2 (4.9)	11.2 (1.9)
	Cropland	0–6	1.25 (2.48)	15.1 (6.4)	28.9 (1.0)	12.9 (1.4)	16.0 (0.8)
		30–36	1.38 (10.55)	10.0 (39.8)	31.2 (7.6)	9.8 (24.4)	21.4 (0.5)
Sep 2012	Forest	0–6	1.10 (9.33)	18.1 (15.8)	31.1 (3.4)	18.2 (2.7)	12.9 (9.5)
		30–36	1.42 (4.62)	12.0 (26.5)	28.0 (10.8)	14.0 (19.8)	14.0 (4.8)
	Grassland	0–6	1.07 (1.68)	20.7 (22.8)	26.9 (1.4)	11.7 (3.2)	15.1 (1.1)
		30–36	1.36 (5.19)	17.4 (8.5)	26.0 (4.0)	14.0 (3.4)	12.0 (4.8)
	Cropland	0–6	1.18 (3.16)	14.2 (18.7)	28.7(3.9)	13.2 (8.7)	15.6 (2.1)
		30–36	1.37 (3.00)	14.1 (23.0)	32.7 (3.0)	12.0 (7.9)	20.8 (0.2)
March 2013	Forest	0–6	1.14 (3.59)	19.7 (20.4)	24.6 (6.9)	11.6 (16.6)	13.0 (4.6)
		30–36	1.26 (0.31)	19.9 (7.6)	28.0 (2.9)	15.7 (6.0)	12.4 (1.1)
	Grassland	0–6	1.24 (3.65)	17.5 (12.0)	27.1 (6.7)	9.7 (18.9)	17.5 (2.3)
		30–36	1.31 (1.93)	17.6 (1.8)	27.1 (0.5)	15.5 (2.2)	11.6 (1.8)
	Cropland	0–6	1.13 (4.08)	22.7 (10.5)	26.3 (2.9)	12.0 (7.2)	14.3 (3.7)
		30–36	1.43 (4.01)	10.5 (31.4)	31.9 (4.1)	10.3 (7.2)	21.6 (4.5)

Table 4: ANOVA tests of between-subjects effects with two factors of land use and time. Hydraulic conductivity at applied pressure heads of 0, –1, –2, –3, –100, –300, –500, –700, and –1000 cm are written as Ksat, K-1, K-2, K-3, K-100, K-300, K-500, K-700, and K-1000. BD = bulk density, AC = air capacity, FC = field capacity, PAWC = plant-available water capacity, PWP = permanent wilting point, Contribution = the contribution of macropore to the flow. DF = degrees of freedom, F = variance of the group means / mean of the within group variances. Sig = Significance value. Significance values < 0.05 indicate that samples from different land uses or measuring time are significantly different at the 5% probability.

Source	Dependent variable	0 cm			30 cm		
		df	F	Sig	df	F	Sig
Land use	Ksat	2	11.396	0.000	2	12.934	0.000
	K-1	2	15.759	0.000	2	12.511	0.000
	K-2	2	17.511	0.000	2	11.464	0.000
	K-3	2	16.975	0.000	2	10.297	0.000
	K-100	2	1.302	0.287	2	2.316	0.117
	K-300	2	2.309	0.117	2	0.150	0.862
	K-500	2	3.107	0.059	2	0.010	0.990
	K-700	2	3.273	0.052	2	0.028	0.973
	K-1000	2	3.172	0.056	2		0.939
	BD	2	1.966	0.155	2	3.195	0.054
	AC	2	1.429	0.254	2	8.614	0.001
	FC	2	3.591	0.039	2	19.424	0.000
	PAWC	2	17.186	0.000	2	20.513	0.000
	PWP	2	11.687	0.000	2	533.810	0.000
	Macroporosity	2	7.817	0.001	2	10.784	0.000
	Contribution	2	7.273	0.002	2	0.564	0.573
Time	Ksat	2	6.900	0.003	2	0.001	0.999
	K-1	2	4.853	0.013	2	0.010	0.990
	K-2	2	3.452	0.041	2	0.036	0.965
	K-3	2	2.657	0.082	2	0.048	0.953
	K-100	2	0.531	0.593	2	0.987	0.385
	K-300	2	0.487	0.619	2	0.308	0.738
	K-500	2	0.747	0.482	2	0.163	0.850
	K-700	2	0.747	0.482	2	0.256	0.776
	K-1000	2	0.667	0.521	2	0.505	0.609
	BD	2	1.596	0.217	2	0.741	0.484
	AC	2	0.385	0.683	2	0.284	0.747
	FC	2	5.292	0.010	2	0.480	0.623
	PAWC	2	5.977	0.006	2	0.067	0.936
	PWP	2	0.583	0.564	2	0.426	0.657
	Macroporosity	2	6.352	0.004	2	0.091	0.913
	Contribution	2	4.755	0.030	2	1.260	0.294

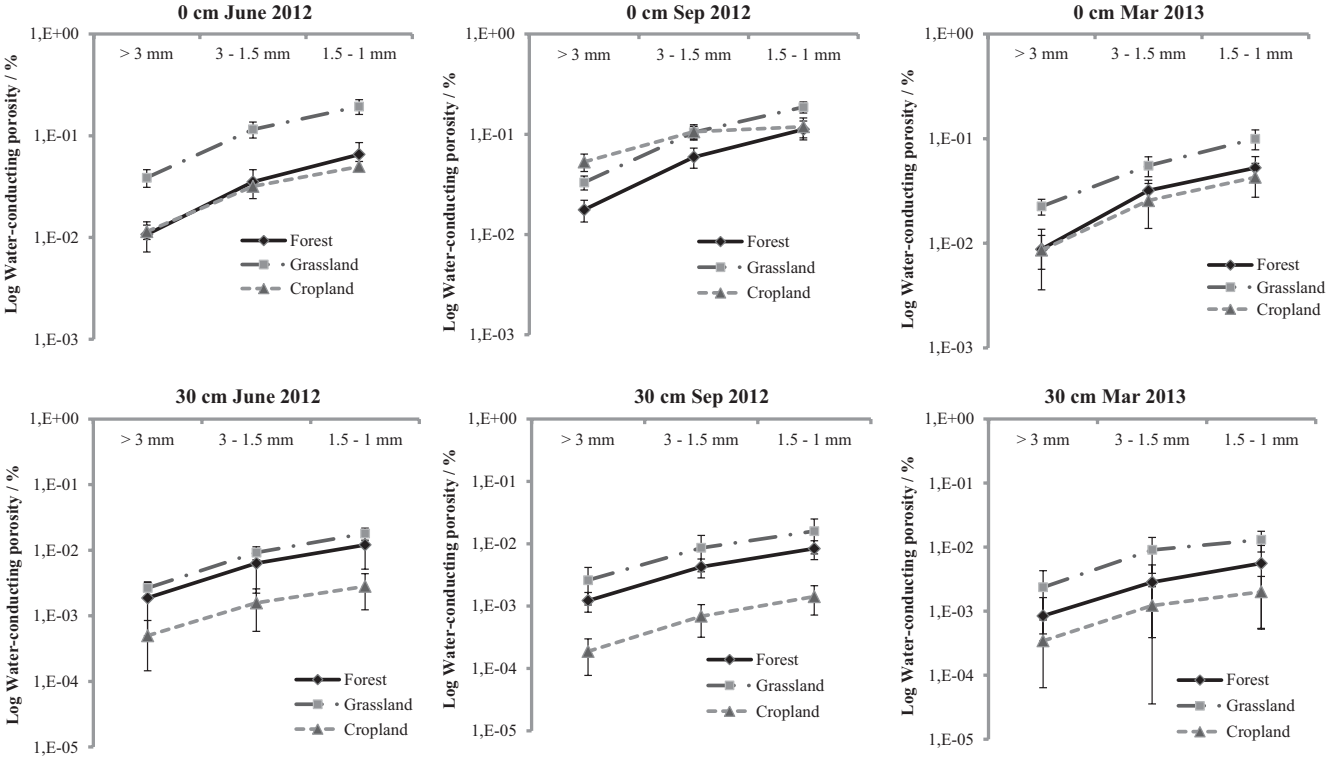

Figure 3: Water-conducting porosity in each pore diameter interval for different plant covers at different measuring times. The vertical bars on the graph represent the standard deviation of five parallel measurements.

conditions of the soil fauna. This increased biological activity may have loosened the soil. The soil under cropping was tilled at the beginning of September 2012. The relatively large conductivity (> 2000 cm d^{-1}) observed at the end of September reflects the loosening effect of tillage. In contrast to September 2012, a significant decrease of the topsoil saturated conductivity was observed under cultivation in June 2012 (801 cm d^{-1}) and in March 2013 (756 cm d^{-1}; Table 2). In comparison, the saturated and near-saturated hydraulic conductivity of subsoil did not differ significantly over the seasons. Analysis indicated that the soil under 30 cm was less sensitive to the change of natural environmental conditions (due to seasonal rainfall, root growth and decay, and structural pore space dynamics) or farming practice.

For both topsoil and subsoil, a high small-scale variability in saturated and near-saturated hydraulic conductivity was found (Table 2). The coefficients of variation (CV) ranged from 14% to 63% in the topsoil, in the subsoil from 30% to 145%, which agrees with other field studies (*Schwärzel* and *Punzel*, 2007; *Hu* et al., 2009; *Schwärzel* et al., 2011). Note that the mean subsoil CV of the saturated and near-saturated hydraulic conductivity of cropland was substantially lower than those of grass or forest. This suggests that regular tillage (30 cm) created a more homogeneous subsoil structure in contrast to the subsoil under grass or forest due to destruction of continuous macropores.

In the topsoil, the water-conducting macroporosity (pore diameter > 1 mm) showed a lowest value of 0.08% (sum) in cropland and highest value of 0.35% in grassland (Fig. 3). In the subsoil, it was 0.002% under cropland and 0.03% under grassland. In general, we can see that the grassland had more macropores than forest and cropland in both topsoil and subsoil. This can be attributed to the abundant biological activities and fine root in the topsoil, as well as no soil compaction in the subsoil. Forest and cropland had a similar macroporosity in the topsoil except for data from September 2012. The exception was mainly caused by plowing after the harvest. In the subsoil, the differences between grassland and forest were less, while they were greater between forest and cropland. However, grassland and forest still showed higher macroporosity than cropland. This is a result of long-term plowing leading to soil compaction under the crop and clogging of the pores. The conventional tillage temporarily increased large pores in the topsoil, but the macroporosity was easily damaged by intense rain or shrinking and swelling of the soil due to poor structure and instability (*Cameira* et al., 2003; *Hu* et al., 2009). Overall, grassland soils had a much higher conductivity than forest soil. The grassland in Zhonggou originates mainly from abandoned arable land, which means the topsoil was quite loose and rich in fine roots even together with the former crops that remained. The hydraulic properties of the subsoil were measured at a depth of 30 cm; at this depth the fine roots of grass were still abundant while the ones of forest were much less. In addition, digging pits on the flat and gentle slopes, or arrangement of the scales of a fish (*i.e.*, semicircular rainwater retention basins arranged as fish scales on steeper slopes) are common techniques for afforestation on the Loess Plateau (*Wang* et al., 2014). By doing so, the soil is compressed while refilling thus leading to the destruction of original structure. This can also partly

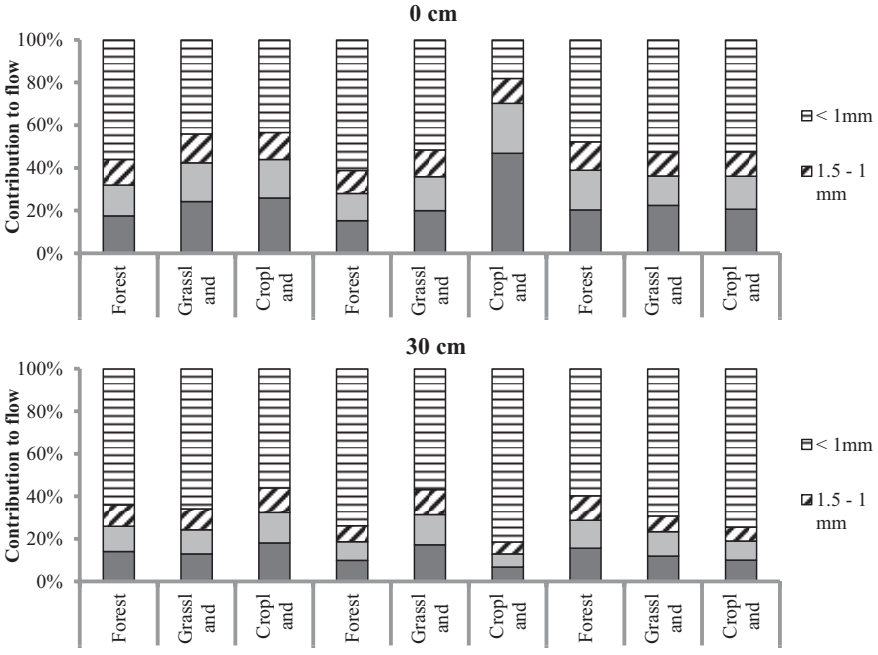

Figure 4: Contribution of each pore class to the flow under forest, grassland, and cropland in June and September 2012 and March 2013. The top graph shows the topsoil data, below the data of the soil depth at 30 cm.

contribute to the low conductivity under forest. *Bodhinayake* and *Cheng Si* (2004) also found for fine loamy soil that the water-conducting macroporosity (pores with diameter > 1 mm) ranged from 0.01% (cultivated land) to 0.04% (native grassland), which are comparable to our results.

The contribution of different pore classes to flow is presented in Fig. 4. Although the macropores consisted of only 0.08–0.35% of the total soil volume (Fig. 3), they conducted up to 80% of the flow under forest, grassland, and cropland (Fig. 4). During the study period, the contribution of pores with diameter > 1 mm did not show significant differences between forest and grassland. For cropland, the total water flow of topsoil was significantly larger in September as compared to that in June and March, accounting for more than 80% of the total flow. Nevertheless, the contribution of this pore class decreased to 47.5% in March (Fig. 4). This was attributed to the effects of plowing (loosening topsoil structure).

3.2 Unsaturated hydraulic conductivity

The results of unsaturated hydraulic conductivity are given in Table 2. No significant differences in unsaturated hydraulic conductivity between the different land-use treatments were identified at a 5% probability. This is not surprising because as suction increases, the influence of soil structure on unsaturated hydraulic conductivity gradually diminishes. It is well accepted that at higher soil suction (*i.e.*, pressure heads < –300 cm) and soil hydraulic properties depend rather on soil texture than on soil structure. Our conductivity data listed in Table 2 reflect this very well. Hence, the impact of different land-use management on the drier part of the unsaturated hydraulic conductivity function (pressure heads < –300 cm), is negligible, at least in this study. Finally, our conductivity data are in line with the findings of other studies, for instance *Zhang* (2005).

3.3 Water retention

The water-retention functions obtained by fitting the van Genuchten–Mualem (VGM) model to the measured water retention data were very similar at first sight, with respect to the shape of the topsoil and partly to the shape of the subsoil water retention curves (Fig. 5). The similarity indicates that the land cover had—under the same soil and weather conditions (at least in this study)—only a minor impact on pore-size distribution. However, differences between the treatments exist in terms of soil water limits as air capacity (AC), field capacity (FC), or plant-available water capacity (PAWC, Table 5). As discussed in section 3.1, grassland promoted the creation of larger macropores which is also indicated by the increased AC in comparison to forest or crops. In contrast, forest tended to promote the formation of mesopores as indicated by the higher PAWC compared to grassland or cropland. This seems to be contradictory to other studies because it is generally accepted that surface horizons of forests soils contain continuous channels or pipe networks mostly formed by soil fauna and active and decaying plant roots (*Moore* et al., 1986). This is also true for the afforested soils of the Loess Plateau but the created macropore system under forest seems to be less stable than the macropore system under grassland. What might be the reason for this phenomenon? The established forests in the Loess Plateau are generally not very dense; therefore, the afforestation consists mostly of understory and overstory. For that reason the seasonal root water uptake under forests is significantly higher than under grassland which means that soils under forest undergo more pronounced drying and wetting cycles in comparison to the soils under grassland. As a result of more intense shrink-swell cycles, more macropores may collapse under forest than under grass. Such a collapse of macropores results in a shift of pore-size distribution towards smaller pores as shown by *Schwärzel* et al. (2011). In comparison to forest and grassland, the topsoil under cropland had the highest permanent

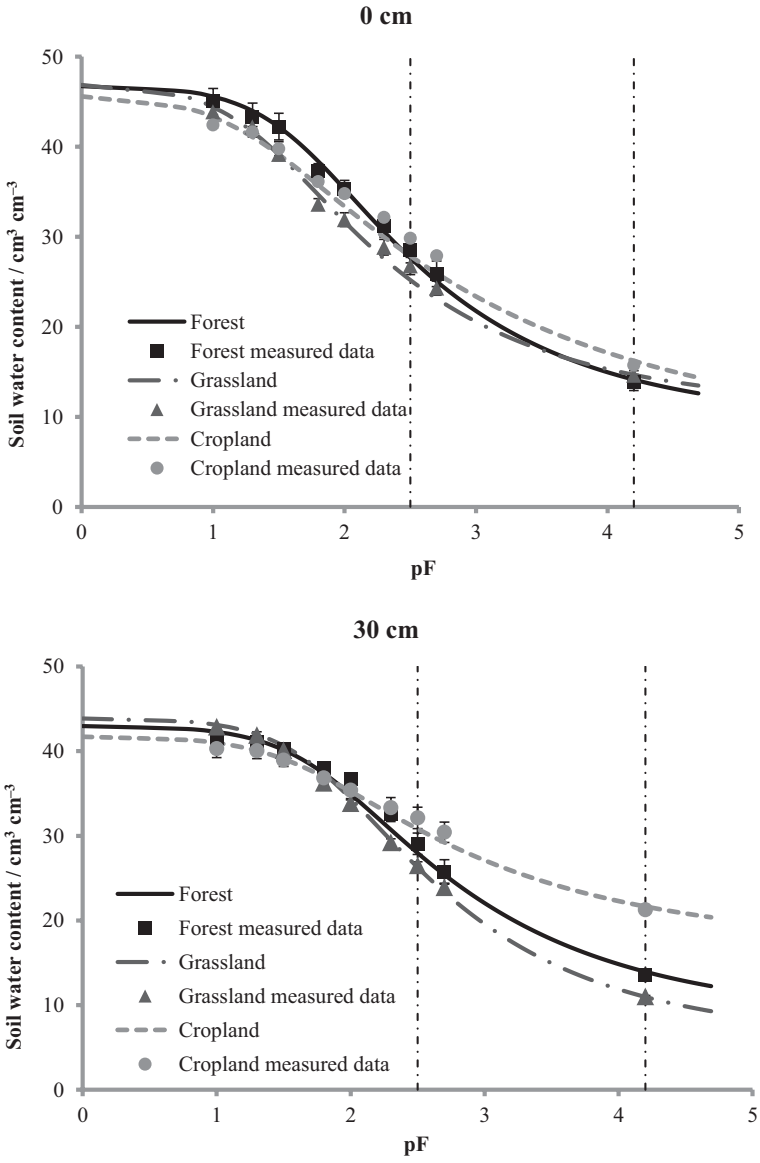

Figure 5: Soil water-retention curves under forest, grassland, and cropland for samples taken in June 2012. The top graph shows the topsoil curves, below the curves of the soil depth at 30 cm. The vertical dashed lines indicate the values at field capacity (pF 2.5) and at the permanent wilting point (pF 4.2). pF = log (|soil pressure head|). The vertical bars on the graph represent the standard deviation of five parallel measurements.

wilting point (PWP) suggesting that cropping may have led to compaction in which the presence of mesopores was reduced and micropores tended to increase. This trend was found to be much more pronounced in the subsoil. Subsoil compactions due to cropping and possible clay translocation resulted in increased bulk density and microporosity at the expense of mesoporosity.

4 Implications for land management

Soil erosion is a severe environmental problem on the Loess Plateau. Intensively cultivated slope farmland was considered as the main factor associated with this problem (*Shi* and *Shao*, 2000). To improve the environmental quality, the Chinese government launched the "Grain for Green" project to return the arable land to forest and grassland (*Wang* et al., 2011). Forest and grassland modify the characteristics of the ground surface and reduce the kinetic energy of the rainfall so that the soil erosion can be reduced during rainstorms. At the same time, the soil water retention has been improved. Many studies have stated that afforestation is an effective measure against soil erosion by stabilizing slope soil in addition to many other benefits, such as alleviate floods, expand carbon sequestration, supply woody products, and allow natural secondary succession (*Sun* et al., 2006; *Zhang* et al., 2014).

Our study indicates that grass may be more capable in improving soil structure and hydraulic conductivity than the black locust type of forest vegetation restoration and afforestation increased infiltration and macropore connectivity. However, forest tended to promote mesopores and therefore the water storage capacity, while grassland promoted the stability of macropores, and therefore the capacity to transmit water rather than to store it. Black locust is the most widely afforested tree species on the Loess Plateau, however, has a very low average survival rate (≈ 38%) and "small-aged" appearance (*Wang* et al., 2014). This implies that although afforesta-

Table 5: Parameter values obtained from the fit of the van Genuchten model [Eq. (6)]. θs = saturated water content, θr = residual water content, α and n are parameters of van Genuchten model.

Measuring Time	Land use	Depth / cm	θs / cm^3 cm^{-3}	θr	α / cm^{-3}	n / –
June 2012	Forest	0	0.481	0.087	0.021	1.324
		30	0.420	0.108	0.008	1.519
	Grassland	0	0.469	0.096	0.047	1.319
		30	0.444	0.041	0.022	1.296
	Cropland	0	0.440	0.078	0.029	1.240
		30	0.413	0.142	0.016	1.287
Sep 2012	Forest	0	0.492	0.083	0.011	1.452
		30	0.400	0.075	0.012	1.372
	Grassland	0	0.446	0.092	0.037	1.297
		30	0.433	0.057	0.022	1.316
	Cropland	0	0.430	0.084	0.039	1.159
		30	0.468	0.144	0.024	1.293
March 2013	Forest	0	0.443	0.109	0.017	1.520
		30	0.479	0.086	0.015	1.443
	Grassland	0	0.450	0.128	0.028	1.456
		30	0.447	0.076	0.014	1.414
	Cropland	0	0.479	0.074	0.056	1.271
		30	0.424	0.193	0.009	1.488

tion promotes infiltration and water storage capacity, insufficient rainwater supply may limit the long-term forest growth. Many studies have reported soil water depletion in deep soil on the Loess Plateau due to artificial plantation (*Chen* et al., 2008; *Jin* et al., 2011) and its substantial impact on water yield and groundwater recharge reduction (*Gates* et al., 2011; *Wang* et al., 2011; *Zhang* et al., 2014). Therefore, from the perspective of water-resources management in a water-limited region, grass might be a more suitable option for soil conservation as it is able to improve macropores and promote water vertical transmission.

5 Conclusions

Our study at pedologically comparable sites of the Loess Plateau revealed that the type of land use had a considerable effect on soil hydraulic conductivity and to a lesser extent on the water retention characteristics of both topsoil and subsoil. Cropping with tillage creates temporary macropores in the topsoil and leads to compaction, loss of macropores and mesopores in the subsoil as indicated by reduced AC, Ksat and PAWC but greater PWP. Our findings suggest that afforestation and grassland had considerable effects on soil structure in which forest tended to promote soil water-storage capacity, whilst grassland promoted infiltration capacity. It has also to be noted that land use change may have substantial impact on water resources depending on the characteristics of the land cover and thus must be considered in initiating an efficient site-specific water management and land-use development scheme on the Loess Plateau.

Acknowledgment

This study was funded by the *Deutsche Forschungsgemeinschaft* (*DFG*) (*SCHW1448–3/1*), the *National Natural Science Foundation of China* (*NSFC*) (*41230852, 41171421*), and the *China Scholarship Council* (*CSC*) for supporting the first author. We would like to thank the *Institute of Soil and Water Conservation in Pingliang* (Gansu Province) for logistic and scientific assistance during the field campaigns. Special thanks to *Trey Monts* for improving the language. Finally, we would like to thank the two anonymous reviewers and Dr. *Horst Gerke*. Their work helped to improve our manuscript significantly.

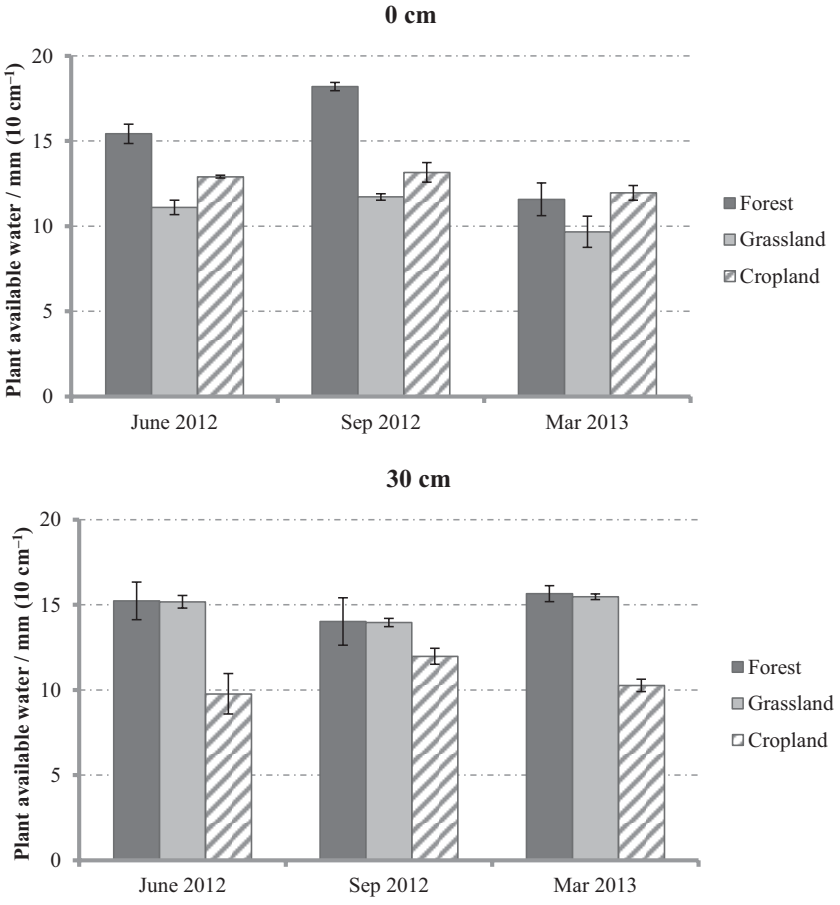

Figure 6: Plant-available water capacity (PAWC) under forest, grassland, and cropland in June and September 2012 and March 2013. The top graph shows the topsoil data, below the data of the soil depth at 30 cm. The vertical bars on the graph represent the standard deviation of five parallel measurements.

References

Angulo-Jaramillo, R., *Vandervaere, J.-P.*, *Roulier, S.*, *Thony, J.-L.*, *Gaudet, J.-P.*, *Vauclin, M.* (2000): Field measurement of soil surface hydraulic properties by disc and ring infiltrometers: A review and recent developments. *Soil Till. Res.* 55, 1–29.

Bodhinayake, W., *Cheng Si, B.* (2004): Near-saturated surface soil hydraulic properties under different land uses in the St. Denis National Wildlife Area, Saskatchewan, Canada. *Hydrol. Process.* 18, 2835–2850.

Boix-Fayos, C., *Calvo-Case, A.*, *Imeso, A. C.*, *Soriano-Soto, M. D.* (2001): Influence of soil properties on the aggregation of some Mediterranean soils and the use of aggregate size and stability as land degradation indicators. *Catena* 44, 47–67.

Cameira, M. R., *Fernando, R. M.*, *Pereira, L. S.* (2003): Soil macropore dynamics affected by tillage and irrigation for a silty loam alluvial soil in southern Portugal. *Soil Till. Res.* 70, 131–140.

Cao, S. X. (2008): Why large-scale afforestation efforts in China have failed to solve the desertification problem. *Environ. Sci. Technol.* 42, 1826–1831.

Chen, H., *Shao, M.*, *Li, Y.* (2008): Soil desiccation in the Loess Plateau of China. *Geoderma* 143, 91–100.

Gardner, W. R. (1958): Some steady-state solutions to the unsaturated moisture flow equation with application to the evaporation from a water table. *Soil Sci.* 85, 228–232.

Gates, J. B., *Scanlon, B. R.*, *Mu, X. M.*, *Zhang, L.* (2011): Impacts of soil conservation on groundwater recharge in the semi-arid Loess Plateau, China. *Hydrogeol. J.* 19, 865–875.

Hu, W., *Shao, M. A.*, *Wang, Q. J.*, *Fan, J.*, *Horton, R.* (2009): Temporal changes of soil hydraulic properties under different land uses. *Geoderma* 149, 355–366.

Hu, W., *Shao, M. A.*, *Si, B. C.* (2012): Seasonal changes in surface bulk density and saturated hydraulic conductivity of natural landscapes. *Eur. J. Soil Sci.* 63, 820–830.

Jin, T. T., *Fu, B. J.*, *Liu, G. H.*, *Wang, Z.* (2011): Hydrologic feasibility of artificial forestation in the semi-arid Loess Plateau of China. *Hydrol. Earth Syst. Sci. Discuss.* 8, 653–680.

Moore, I. D., *Burch, G. J.*, *Wallbrink, P. J.* (1986): Preferential flow and hydraulic conductivity of forest soils. *Soil Sci. Soc. Am. J.* 50, 876–881.

Mualem, Y. (1976): A new model for predicting the hydraulic conductivity of unsaturated porous media. *Water Resour. Res.* 12, 513–522.

Reynolds, W. D., *Zebchuk, W. D.* (1996): Use of contact material in tension infiltrometer instruments. *Soil Technol.* 9, 141–159.

Scheffler, R., *Neill, C.*, *Krusche, A. V.*, *Elsenbeer, H.* (2011): Soil hydraulic response to land-use change associated with the recent soybean expansion at the amazon agricultural frontier. *Agr. Ecosyst. Environ.* 144, 281–289.

Schindler, U. (1980): Ein Schnellverfahren zur Messung der Wasserleitfähigkeit im teilgesättigten Boden an Stechzylinderproben. *Arch. Acker. Pfl. Boden.* 24, 1–7.

Schwärzel, K., *Carrick, S.*, *Wahren, A.*, *Feger, K. H.*, *Bodner, G.*, *Buchan, G.* (2011): Soil hydraulic properties of recently tilled soil under cropping rotation compared with 2-years-pasture: Measurement and modeling the soil structure dynamics. *Vadose Zone J.* 11, 354–366.

Schwärzel, K., *Punzel, J.* (2007): Hood infiltrometer—a new type of tension infiltrometer. *Soil Sci. Soc. Am. J.* 71, 1438–1447.

Schwärzel, K., *Simunek, J.*, *Stoffregen, H.*, *Wessolek, G.*, *van Genuchten, M. T.* (2006): Estimation of the unsaturated hydraulic conductivity of peat soils: Laboratory versus field data. *Vadose Zone J.* 5, 628–640.

Shi, H., *Shao, M. A.* (2000): Soil and water loss from the Loess Plateau in China. *J. Arid Environ.* 45, 9–20.

Shukla, M. K., *Lal, R.*, *Owens, L. B.*, *Unkefer, P.* (2003): Land use and management impacts on structure and infiltration characteristics of soil in the north Appalachian region of Ohio. *Soil Sci.* 168, 167–177.

Springer, E. P., *Cundy, T. W.* (1988): The effect of spatial-varying soil properties on soil erosion. Proceedings of the 1988 International Symposium "Modelling Agricultural, Forest, and Rangeland Hydrology". ASAE Publication, St. Joseph, MI, USA, pp. 281–296.

Stolte, J., *Venrooij, B. V.*, *Zhang, G. H.*, *Trouwborst, K. O.*, *Liu, G. B.*, *Ritsema, C. J.*, *Hessel, R.* (2003): Land-use induced spatial heterogeneity of soil hydraulic properties on the Loess Plateau in China. *Catena* 54, 59–75.

Sun, G., *Zhou, G.*, *Zhang, Z.*, *Wie, X.*, *McNulty, S. G.*, *Vose, J. M.* (2006): Potential water yield reduction due to forestation across China. *J. Hydrol.* 328, 548–558.

van Genuchten, M. T. (1980): A closed-form equation for predicting the hydraulic conductivity of unsaturated soils. *Soil Sci. Soc. Am. J.* 44, 892–898.

Wang, L., *Wei, S. P.*, *Horton, R.*, *Shao, M. A.* (2011): Effects of vegetation and slope aspect on water budget in the hill and gully region of the Loess Plateau of China. *Catena* 87, 90–100.

Wang, Y., *Yu, P.*, *Feger, K.-H.*, *Wei, X.*, *Sun, G.*, *Bonell, M.*, *Xiong, W.*, *Zhang, S.*, *Xu, L.* (2011): Annual runoff and evapotranspiration of forestlands and non-forestlands in selected basins of the Loess Plateau of China. *Ecohydrology* 4, 277–287.

Wang, Z., *Jiao, J.*, *Su, Y.*, *Chen, Y.* (2014): The efficiency of large-scale afforestation with fish-scale pits for revegetation and soil erosion control in the steppe zone on the hill-gully Loess Plateau. *Catena* 115, 159–167.

Watson, K., *Luxmoore, R.* (1986): Estimating macroporosity in a forest watershed by use of a tension infiltrometer. *Soil Sci. Soc. Am. J.* 50, 578–582.

Wooding, R. A. (1968): Steady infiltration from a shallow circular pond. *Water Resour. Res.* 4, 1259–1273.

WRB (2006): World Reference Base for Soil Resources. FAO, Rome, Italy.

Zhang, G. S., *Chan, K. Y.*, *Li, G. D.*, *Huang, G. B.* (2011): The effects of stubble retention and tillage practices on surface soil structure and hydraulic conductivity of a loess soil. *Acta Ecol. Sin.* 31, 298–302.

Zhang, L., *Podlasly, C.*, *Ren, Y.*, *Feger, K.-H.*, *Wang, Y.*, *Schwärzel, K.* (2014): Separating the effects of changes in land management and climatic conditions on long-term streamflow trends analyzed for a small catchment in the Loess Plateau region, NW China. *Hydrol. Process.* 28, 1284–1293.

Zhang, S. L. (2005): Soil hydraulic properties and water balance under various soil management regimes on the Loess Plateau, China. PhD thesis, Swedish University of Agricultural Science, Umeå, Sweden.

Zhang, S. L., *Lövdahl, L.*, *Grip, H.*, *Tong, Y.* (2007): Soil hydraulic properties of two loess soils in China measured by various field-scale and laboratory methods. *Catena* 69, 264–273.

Zhang, X., *Quine, T. A.*, *Walling, D. E.* (1998): Soil erosion rates on sloping cultivated land on the Loess Plateau near Ansai, Shaanxi Province, China: an investigation using 137Cs and rill measurements. *Hydrol. Process.* 12, 171–189.

Zhou, D. C., *Zhao, S. Q.*, *Zhu, C.* (2012): The Grain for Green Project induced land cover change in the Loess Plateau: a case study with Ansai County, Shanxi Province, China. *Ecol. Indic.* 23, 88–94.

